

Journal of Biomedical Optics

SPIEDigitalLibrary.org/jbo

Geometry-invariant gradient refractive index lens: analytical ray tracing

Mehdi Bahrami
Alexander V. Goncharov

Geometry-invariant gradient refractive index lens: analytical ray tracing

Mehdi Bahrami and Alexander V. Goncharov

National University of Ireland, Galway, School of Physics, Applied Optics Group, University Road, Galway, Ireland

Abstract. A new class of gradient refractive index (GRIN) lens is introduced and analyzed. The interior iso-indicial contours mimic the external shape of the lens, which leads to an invariant geometry of the GRIN structure. The lens model employs a conventional surface representation using a coinoid of revolution with a higher-order aspheric term. This model has a unique feature, namely, it allows analytical paraxial ray tracing. The height and the angle of an arbitrary incident ray can be found inside the lens in a closed-form expression, which is used to calculate the main optical characteristics of the lens, including the optical power and third-order monochromatic aberration coefficients. Moreover, due to strong coupling of the external surface shape to the GRIN structure, the proposed GRIN lens is well suited for studying accommodation mechanism in the eye. To show the power of the model, several examples are given emphasizing the usefulness of the analytical solution. The presented geometry-invariant GRIN lens can be used for modeling and reconstructing the crystalline lens of the human eye and other types of eyes featuring a GRIN lens. © 2012 Society of Photo-Optical Instrumentation Engineers (SPIE). [DOI: 10.1117/1.JBO.17.5.055001]

Keywords: gradient index lens; crystalline lens; exact ray tracing; lens paradox.

Paper 11690 received Nov. 25, 2011; revised manuscript received Mar. 22, 2012; accepted for publication Mar. 22, 2012; published online May 7, 2012.

1 Introduction

Recent advances in new materials facilitate the application of gradient refractive index (GRIN) lenses in a variety of optical devices, especially in the development of bio-inspired lenses¹ and optical systems. Employing optical elements with a spatially variable index of refraction is a powerful way to achieve improved imaging. The best example of such a GRIN lens is the well-known Luneburg lens,² which is free from all monochromatic aberrations. The crystalline lens in the human eye is another example of a GRIN lens. In the present paper we explore a new mathematical model describing the crystalline GRIN lens. The gradual variation of the refractive index of the crystalline lens has been known for a long time and several models have been developed to account for the GRIN structure.^{3–7} Advances in ocular aberration measurements,⁸ magnetic resonance imaging,^{9,10} optical tomography,¹¹ optical coherence tomography imaging,¹² and X-ray Talbot interferometry¹³ have enabled researchers to improve existing eye models. Using this new data, several research groups have attempted to construct more realistic models of the GRIN lens. Navarro et al. proposed a GRIN lens model with concentric iso-indicial contours mimicking the external conic surfaces of the lens.¹⁴ The GRIN spatial distribution of this model follows the experimental age-dependent formula suggested in earlier work.¹⁵ For the first time, a GRIN lens model features a curved equatorial plane, where anterior and posterior hemispheres meet. Using a different approach, Goncharov and Dainty introduced a wide-field schematic eye model with a GRIN lens, which uses a fourth-order polynomial describing the refractive structure of the lens.¹⁶ Similar to the Navarro model, the external shape of the lens defines its GRIN structure. By estimating a parabolic path for the rays in the human GRIN

lens¹⁷ and using Sands' third-order aberrations study in inhomogeneous lenses,¹⁸ this model presents approximated formulas for the power of the lens and its spherical aberration. Another recent model proposed by Díaz et al. uses a combination of polynomials and trigonometric functions for describing the refractive index distribution.¹⁹ The coefficients of the refractive index of the lens are given as a linear function of age. Both models, Goncharov and Dainty and Díaz et al., are complete eye models providing age-dependent equations for the curvatures of the cornea and lens. Following the Navarro et al. model for the GRIN lens *in vitro*,¹⁴ in a recent work by Castro et al., the power law of the GRIN lens profile has been modified to account for a possible toricity of the lens surface.¹² The variety of eye models featuring different GRIN profiles shows the great interest in lens structure and its effect on optical performance. In spite of the apparent progress made in this area, there is no simple GRIN lens model providing exact paraxial equations for the path of the rays inside the GRIN structure. It would be beneficial to have an analytical way to calculate the power and the third-order aberrations for the lens. Analytical solutions can help researchers gain a better understanding of the GRIN structure role in image formation and simplify the optical analysis of the lens. In addition, if such a model could also provide a more realistic (continuous) geometry of the GRIN lens's iso-indicial contours, it would become a valuable tool for reconstructing the human eye and modeling the accommodation mechanism. In the following section we introduce such a GRIN lens model and outline its main geometrical properties.

2 Parametric Model of the GRIN Lens

2.1 Refractive Index Equation Based on Experimental Data

There are many experimental studies focusing on the distribution of refractive index in the crystalline lens. In 1969 Nakao

Address all correspondence to: Mehdi Bahrami, National University of Ireland, Galway, School of Physics, Applied Optics Group, University Road, Galway, Ireland. Tel: +353 91 495350; Fax: +353 91 495529; E-mail: m.bahrami@nuigalway.ie

et al. suggested a parabolic distribution for the refractive index in all directions:²⁰

$$n(r) = c_0 + c_1 r^2, \quad (1)$$

where c_0 is the refractive index at the center of the lens, c_1 is the difference between the central index and the surface index, and r is a normalized distance from the lens center defining the geometry of the lens. Following this approach, Smith et al.⁶ introduced more terms in Eq. (1) to get a better fit to experimental data.²¹ Later, Smith et al.¹⁵ proposed power-law to describe the distribution of refractive index along the optical axis as:

$$n(r) = c_0 + c_1 r^{2p}, \quad (2)$$

where the parameter p in the exponent is used to account for age-related changes in the GRIN lens. Equation (2) was used by Navarro et al. as a starting point for modeling GRIN lenses *in vitro*.¹⁴ For clarity we rewrite Eq. (2) as

$$n(\zeta) = n_c + (n_s - n_c)(\zeta^2)^p, \quad (3)$$

where ζ is the normalized distance from the center of the lens, n_c and n_s are the refractive indices at the center and at the surface of the GRIN lens, respectively. Here, ζ changes between -1 to $+1$ to cover both anterior and posterior hemispheres of the lens; also we avoid introducing complex numbers by using the form $(\zeta^2)^p$.

2.2 Geometry of Iso-Indicial Contours

From the optical design point of view, it is convenient to describe the external surfaces of the GRIN lens as a conicoid of revolution:

$$z = \frac{c\rho^2}{1 + \sqrt{1 - (1+k)c^2\rho^2}}, \quad (4)$$

where c and k are respectively the curvature and the conic constant of the surface, and ρ is the distance from the optical z axis. There are other possible mathematical representations for the geometry GRIN lens, for example hyperbolic cosines²² or Fourier series of cosines.²³ However these alternative representations do not have a straight forward connection with the radius of curvature and conic constant of the lens surface. On the other hand, using Eq. (4) greatly simplifies the parameterization of the surface. Following the idea of constructing the lens with conic surfaces on both sides,¹⁴ one might get discontinuity of iso-indicial contours in equatorial interface joining two hemispheres. To avoid this problem, one could add an additional term on the right side of Eq. (4). Before we derive the continuity condition for iso-indicial contours at the equatorial interface, it is more convenient to rewrite Eq. (4) as a function of surface sag:

$$\rho^2 = 2rz - (1+k)z^2, \quad (5)$$

where r is the radius of curvature of the surface. Now introducing an additional term on the right side will help achieve the continuity condition. The surface equation becomes as:

$$\rho^2 = 2rz - (1+k)z^2 + bz^3, \quad (6)$$

where b is a constant, which is used to satisfy the continuity condition by making the first derivative $d\rho/dz = 0$ at the equatorial interface connecting the posterior and anterior

hemispheres. Based on this approach, Eq. (7) represents our new description for the surface of iso-indicial contours:

$$\begin{aligned} \rho_a^2 &= 2r_a(t_a + z) - (1 + k_a)(t_a + z)^2 + b_a(t_a + z)^3, \\ -t_a &\leq z < 0 \end{aligned} \quad (7a)$$

$$\begin{aligned} \rho_p^2 &= 2r_p(t_p - z) - (1 + k_p)(t_p - z)^2 + b_p(t_p - z)^3, \\ 0 &\leq z \leq t_p \end{aligned} \quad (7b)$$

where subscripts a and p respectively stand for anterior and posterior parts of the lens, and t is the intercept of the iso-indicial contours measured from the origin O along the optical axis. Figure 1 depicts the continuous contours described by Eq. (7). With these recent techniques one could determine the intercept and the radius of curvature of the external surface, T and R , respectively. Iso-indicial contours plots obtained by Jones et al.⁹ show that the center of curvature of the inner contours gradually shifts toward the center O as a result of their steepening. This effect is more obvious in younger eyes, where central contours are still distinguishable. The simplest way to account for such a gradual change in curvature with depth is to define r as a linear function of the normalized distance from the center, $r = R\zeta$. It is worth noting that for both anterior and posterior hemispheres r , R , t , and T are numerically positive quantities; see Fig. 1.

By using Eq. (3), now we shall derive the continuity condition and find the corresponding refractive index for each iso-indicial contour. To satisfy the continuity condition we have to fulfill two constraints for an iso-indicial contour: zero derivative, $d\rho/dz = 0$, and equal heights, $\rho_a(z_c) = \rho_p(z_c)$, at the joining point z_c , as shown in Fig. 1. Using the first constraint, we determine b_a and b_p . As a result, for both hemispheres of the lens we have:

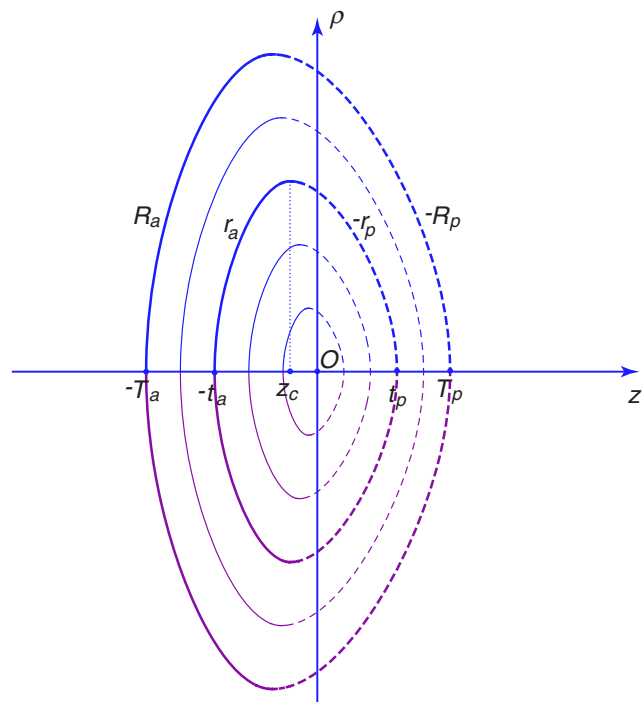


Fig. 1 Iso-indicial shells based on Eq. (7). Solid lines indicate the anterior part of the lens and the dashed lines specify the posterior part.

$$b_a = \frac{2(1+k_a)(t_a+z_c)-r_a}{3(t_a+z_c)^2}, \quad (8a)$$

$$b_p = \frac{2(1+k_p)(t_p-z_c)-r_p}{3(t_p-z_c)^2}. \quad (8b)$$

Using the second constraint we find the coordinate of the joining point as a function of the lens parameters r_a , r_p , k_a , k_p , t_a , and t_p :

$$z_c = \frac{2\eta}{-\mu - \sqrt{\mu^2 - 4\nu\eta}}, \quad (9)$$

where

$$\eta = \frac{1}{3}[-t_a^2(1+k_a) + 4t_a r_a + t_p(-6r_p + t_p(1+k_p)(3+2r_p))],$$

$$\mu = \frac{2}{3}[-t_a(1+k_a) + 2r_a + 3r_p - t_p(1+k_p)(3-t_p(1+k_p) + r_p)],$$

and $\nu = \frac{1}{3}[2-k_a + 3k_p - 2t_p(1+k_p)^2]$.

In the following sections we shall describe the optical properties of this GRIN lens model.

3 Thin Lens Approximation

The optical characteristics of a GRIN lens, such as the optical power and third-order aberrations, are usually not available in analytical form. However, in some cases (e.g., Ref. 24) and for our GRIN lens model it is possible to derive analytical expressions, which are given in Secs. 6 and 7. Although in Sec. 5 we discuss exact paraxial equations, it would be useful to start with a simplified power equation. The optical power of the GRIN lens can be described as the sum of the contributions from three components: the anterior surface of the lens, F_{as} ; the GRIN structure of the lens, F_{GRIN} ; and the posterior surface of the lens, F_{ps} . The optical power for the anterior and the posterior surfaces are given by a conventional equation²⁵

$$F_s = \frac{n_2 - n_1}{R}, \quad (10)$$

where n_1 and n_2 are respectively the refractive indices before and after the surface and R is the radius of curvature. To derive the expression for the optical power arising from the GRIN structure of the lens, we consider the GRIN lens structure as an infinite sum of thin homogeneous shells. Now by adding the power of all shells and considering that their thickness is negligibly small, we can obtain an approximate expression for the lens power. To do this, we rewrite Eq. (10) using the definition of derivative in a continuous medium

$$\delta F_{GRIN} = \frac{n'(\zeta)\delta\zeta}{R}. \quad (11)$$

Using Eq. (3) and taking the integral we find the optical power of the GRIN structure.

$$F_{GRIN} = \int_{-1}^0 \frac{2p(n_s - n_c)(\zeta^2)^{p-\frac{1}{2}}}{-R_a\zeta} d\zeta - \int_0^1 \frac{2p(n_s - n_c)(\zeta^2)^{p-\frac{1}{2}}}{R_p\zeta} d\zeta. \quad (12)$$

Experimental data suggest that for human eyes p is always larger than 2 (e.g., Ref. 14) and therefore Eq. (12) can be simplified to

$$F_{GRIN} = \frac{2p}{2p-1}(n_c - n_s)\left(\frac{1}{R_a} + \frac{1}{R_p}\right). \quad (13)$$

Finally, the total power of the lens is

$$F_{thin} = \frac{n_s - n_{aqu}}{R_a} + \frac{2p}{2p-1}(n_c - n_s)\left(\frac{1}{R_a} + \frac{1}{R_p}\right) + \frac{n_{vit} - n_s}{-R_p}, \quad (14)$$

where n_{aqu} and n_{vit} are respectively the refractive indices of the media before and after the lens.

4 Optical Path Length

One other useful characteristic of an optical element is its optical path length (OPL), defined as the product of the geometric length of the light path and the refractive index of the medium.²⁵ In a GRIN lens the refractive index gradually changes, then the OPL can be calculated as the sum of the small propagations in each infinitely thin iso-indicial shell. Since the paraxial thickness of these thin shells is simply $T_a d\zeta$ and $T_p d\zeta$ for anterior and posterior hemispheres, respectively, using Eq. (3) we can define the paraxial OPL of the presented GRIN model as

$$OPL = \int_{-1}^0 (n_c + (n_s - n_c)(\zeta^2)^p) T_a d\zeta + \int_0^1 (n_c + (n_s - n_c)(\zeta^2)^p) T_p d\zeta, \quad (15)$$

which results

$$OPL = (T_a + T_p) \frac{2n_c p + n_s}{2p + 1}. \quad (16)$$

It is worth mentioning that the geometry of the iso-indicial contours is not contributing to the paraxial OPL of the lens, so Eq. (16) is applicable for any GRIN lens employing the paraxial refractive index distribution in Eq. (3) (e.g., the GRIN lens model proposed by Navarro et al.¹⁴).

5 Analytical Paraxial Ray Tracing

It is notoriously difficult to perform exact ray tracing through a GRIN lens, which is done numerically using optical design software. Even exact paraxial ray tracing equations are not available for GRIN lenses. One could also use an approximate method, where the ray path within the GRIN lens is assumed to be parabolic.¹⁷ However, it would be desirable to have an exact method for paraxial ray tracing so that all optical characteristics of the lens can be found in closed form. Due to the linear dependence of the iso-indicial contours radius r on the normalized axial distance, $\zeta = z/T$, we are able to derive a closed-form solution for paraxial ray tracing in the geometry-invariant GRIN lens. Paraxial ray tracing is based on two main equations.²⁵ According to the first one we have

$$n_2 u_2 = n_1 u_1 - \frac{y_1}{R_1}(n_2 - n_1), \quad (17)$$

where n_1 and n_2 are respectively the refractive indices before and after the interface surface, u_1 and u_2 are the angles of the incident and refracted rays, y_1 is the height of the ray at

the surface, and R_1 is the radius of the surface. For the next surface located at the axial distance d_2 from the first one, the height of the incident ray, y_2 , is obtained by

$$y_2 = y_1 + d_2 u_2. \quad (18)$$

Following the same approach used to derive Eq. (11), we rewrite the axial thickness of the infinitely thin shells as $d_2 = \delta z$, then Eq. (18) becomes

$$u(z) = y'(z). \quad (19)$$

Using Eq. (3) and substituting the definition of the derivative from Eq. (19) into Eq. (17) results in

$$\begin{aligned} n\left(\frac{z+\delta z}{T}\right) \frac{y(z+2\delta z) - y(z+\delta z)}{\delta z} \\ = n\left(\frac{z}{T}\right) \frac{y(z+\delta z) - y(z)}{\delta z} + \frac{y(z)}{R(z/T)} \left[n\left(\frac{z+\delta z}{T}\right) - n\left(\frac{z}{T}\right) \right]. \end{aligned} \quad (20)$$

Finally considering u and y as continuous functions of z , we expand Eq. (20) around the origin for δz and keep only the first order terms, which gives us

$$\frac{y(z)n'(z/T)}{Rz} - \frac{n'(z/T)y'(z)}{T} - n(z/T)y''(z) = 0. \quad (21)$$

Solving Eq. (21) for the anterior and posterior hemispheres (where T corresponds to T_a and T_p , respectively) leads to a general ray equation:

$$y(z) = \begin{cases} c_{12} F_1 \left[\frac{-1+2p-\alpha}{4p}, \frac{-1+2p+\alpha}{4p}; 1 - \frac{1}{2p}; \frac{n_c - n_s}{n_c} \left(\frac{-z}{T_a}\right)^{2p} \right] \\ + z \frac{c_2}{T_a} {}_2F_1 \left[\frac{1+2p-\alpha}{4p}, \frac{1+2p+\alpha}{4p}; 1 + \frac{1}{2p}; \frac{n_c - n_s}{n_c} \left(\frac{-z}{T_a}\right)^{2p} \right] & -T_a \leq z < 0 \\ c_{12} F_1 \left[\frac{-1+2p-\beta}{4p}, \frac{-1+2p+\beta}{4p}; 1 - \frac{1}{2p}; \frac{n_c - n_s}{n_c} \left(\frac{z}{T_p}\right)^{2p} \right] \\ + z \frac{c_2}{T_a} {}_2F_1 \left[\frac{1+2p-\beta}{4p}, \frac{1+2p+\beta}{4p}; 1 + \frac{1}{2p}; \frac{n_c - n_s}{n_c} \left(\frac{z}{T_p}\right)^{2p} \right] & 0 \leq z \leq T_p, \end{cases} \quad (22)$$

where ${}_2F_1$ is Gaussian (ordinary) hypergeometric function and

$$\alpha = \sqrt{8T_a p / R_a + (1 - 2p)^2}$$

$$\beta = \sqrt{8T_p p / R_p + (1 - 2p)^2}$$

$$c_1 = -\frac{\mathcal{F}_2 T_a u_0 + y_0 (\mathcal{F}_5 + \mathcal{F}_4 \gamma_1)}{\mathcal{F}_2 \mathcal{F}_3 \gamma_2 - \mathcal{F}_1 (\mathcal{F}_5 + \mathcal{F}_4 \gamma_1)}$$

$$c_2 = -\frac{y_0}{\mathcal{F}_2} + \frac{\mathcal{F}_1}{\mathcal{F}_2} c_1,$$

where u_0 and y_0 are respectively the angle and the height of the incident ray after refraction by the anterior surface of the lens and the expressions for \mathcal{F}_i and γ_j are given in the appendix. Using Eqs. (19) and (22), the angle of the ray can be found as

$$u(z) = \begin{cases} \frac{c_1}{T_a} \gamma_2 \left(\frac{-z}{T_a}\right)^{2p-1} {}_2F_1 \left[\frac{-1+6p+\alpha}{4p}, \frac{-1+6p-\alpha}{4p}; 2 - \frac{1}{2p}; \frac{n_c - n_s}{n_c} \left(\frac{-z}{T_a}\right)^{2p} \right] \\ + \frac{c_2}{T_a} \gamma_1 \left(\frac{-z}{T_a}\right)^{2p} {}_2F_1 \left[\frac{1+6p-\alpha}{4p}, \frac{1+6p+\alpha}{4p}; 2 + \frac{1}{2p}; \frac{n_c - n_s}{n_c} \left(\frac{-z}{T_a}\right)^{2p} \right] & -T_a \leq z < 0 \\ + \frac{c_2}{T_a} {}_2F_1 \left[\frac{1+2p-\alpha}{4p}, \frac{1+2p+\alpha}{4p}; 1 + \frac{1}{2p}; \frac{n_c - n_s}{n_c} \left(\frac{-z}{T_a}\right)^{2p} \right] \\ \frac{c_1}{T_p} \gamma_4 \left(\frac{z}{T_p}\right)^{2p-1} {}_2F_1 \left[\frac{-1+6p+\beta}{4p}, \frac{-1+6p-\beta}{4p}; 2 - \frac{1}{2p}; \frac{n_c - n_s}{n_c} \left(\frac{z}{T_p}\right)^{2p} \right] \\ + \frac{c_2}{T_a} \gamma_3 \left(\frac{z}{T_p}\right)^{2p} {}_2F_1 \left[\frac{1+6p-\beta}{4p}, \frac{1+6p+\beta}{4p}; 2 + \frac{1}{2p}; \frac{n_c - n_s}{n_c} \left(\frac{z}{T_p}\right)^{2p} \right] & 0 \leq z \leq T_p. \\ + \frac{c_2}{T_a} {}_2F_1 \left[\frac{1+2p-\beta}{4p}, \frac{1+2p+\beta}{4p}; 1 + \frac{1}{2p}; \frac{n_c - n_s}{n_c} \left(\frac{z}{T_p}\right)^{2p} \right] \end{cases} \quad (23)$$

Both the height $y(z)$ and the angle $u(z)$ of the ray are necessary to describe the optical properties of the GRIN lens, which is the main goal of Secs. 6 and 7.

It is worth mentioning that the tilt or decenter of the lens can be seen as a change in the angle and the height of the incident ray, respectively, and Eqs. (22) and (23) are still applicable.

6 Analytical Expression for Optical Power

In this section we present an analytical expression for the optical power of the GRIN lens derived with the help of Eqs. (22) and (23). First we consider the power of a homogeneous lens:²⁵

$$F_L = \frac{(n_2 - n_1)}{R_1} - \frac{(n_2 - n_3)}{R_2} + d \frac{(n_2 - n_3)(n_2 - n_1)}{n_2 R_1 R_2}, \quad (24)$$

where n_1 , n_2 , and n_3 are respectively the refractive indices of the medium before the lens, within the lens, and the medium after the lens; d is the thickness of the lens, and R_1 and R_2 are respectively the radius of curvatures for the anterior and posterior surfaces. Equation (24) is derived from Eqs. (17) and (18). Using a similar approach, Eqs. (22) and (23) will give the optical power of the GRIN lens

$$F = A_a \frac{(n_s - n_{\text{aqu}})}{R_a} + A_{\text{GRIN}} - A_p \frac{(n_s - n_{\text{vit}})}{-R_p} + A_d \frac{(n_s - n_{\text{vit}})(n_s - n_{\text{aqu}})}{-n_s R_a R_p}, \quad (25)$$

where A_a , A_{GRIN} , A_p , and A_d are constants associated with the GRIN structure of the lens, the expressions of which are given in Appendix. For a simple lens, where $n_s = n_c$, it can be shown that $A_a = 1$, $A_{\text{GRIN}} = 0$, $A_p = 1$, and $A_d = T_a + T_p$, which reduces Eq. (25) to Eq. (24). On the other hand, by assuming t_a and t_p are small enough to be ignored, we get $A_a = 1$, $A_{\text{GRIN}} = F_{\text{GRIN}}$, $A_p = 1$, and $A_d = 0$, which simplifies Eq. (25) to Eq. (14).

Using Eq. (25), we can find the focal length, f , and the back focal length of the lens, f_{back} as

$$f = \frac{n_{\text{vit}}}{F}, \quad (26)$$

and

$$f_{\text{back}} = f B_f, \quad (27)$$

where B_f is defined in the Appendix.

We shall stress that the optical power of the lens is not affected by its tilt or decenter and remains one of the fundamental characteristics of the lens.

7 Third-Order Aberrations

In general, the contribution of a GRIN lens to Seidel aberrations can be divided in two parts. The first part is the surface contribution of the interface between the homogeneous medium and inhomogeneous (GRIN) medium. The second part is the transfer contribution originating inside the GRIN media. For a GRIN lens with iso-indicial contours being coincident with the external surfaces, the surface contribution can be calculated as a conventional contribution from an interface between homogeneous media. Therefore we shall start with a single surface

contribution to the primary third-order monochromatic aberrations. The coefficient of third-order spherical aberration is given by²⁶

$$S_I = -y \left[\left(\frac{u_2 - u_1}{1/n_2 - 1/n_1} \right)^2 \left(\frac{u_2}{n_2} - \frac{u_1}{n_1} \right) + k \frac{(n_2 u_2 - n_1 u_1)^3}{(n_2 - n_1)^2} \right], \quad (28)$$

where y is the height of the marginal ray at the surface, u_1 and u_2 are respectively the incident and refracted rays angles relative to the optical axis, n_1 and n_2 are respectively the refractive indices before and after the surface, and k is the conic constant of the surface. Similar to our derivation of Eq. (20), from Eq. (28) we find the contribution of an infinitely thin layer within the GRIN structure as

$$\delta S_I = -y(z) \left\{ \frac{T n^2(\frac{z}{T}) y'^2(z) [-n'(\frac{z}{T}) y'(z) + T n(\frac{z}{T}) y''(z)]}{n'^2(\frac{z}{T})} + k \frac{[n'(\frac{z}{T}) y'(z) + T n(\frac{z}{T}) y''(z)]^3}{T n'^2(\frac{z}{T})} \right\} \delta z, \quad (29)$$

then by considering the contribution of the anterior and posterior surfaces and summing up all thin layer contributions of the GRIN structure we have

$$\begin{aligned} \sum S_I = & -y_0 \left[\left(\frac{u_0 - u_a}{1/n_s - 1/n_{\text{aqu}}} \right)^2 \left(\frac{u_0}{n_s} - \frac{u_a}{n_{\text{aqu}}} \right) \right. \\ & \left. + k_a \frac{(n_s u_0 - n_{\text{aqu}} u_a)^3}{(n_s - n_{\text{aqu}})^2} \right] \\ & + \int_{-T_a}^{T_p} dS_I - y(T_p) \left\{ \left[\frac{u_p - u(T_p)}{1/n_{\text{vit}} - 1/n_s} \right]^2 \left[\frac{u_p}{n_{\text{vit}}} - \frac{u(T_p)}{n_s} \right] \right. \\ & \left. + k_p \frac{[n_{\text{vit}} u_p - n_s u(T_p)]^3}{(n_{\text{vit}} - n_s)^2} \right\}, \quad (30) \end{aligned}$$

where u_a is the marginal ray angle at the anterior surface and $u(T_p)$ and u_p are the angles of the marginal ray immediately before and after the posterior surface, respectively. The latter can be derived using Eq. (17)

$$u_p = \frac{1}{n_{\text{vit}}} \left[n_s u(T_p) + \frac{y(T_p)}{R_p} (n_{\text{vit}} - n_s) \right]. \quad (31)$$

In addition to the marginal ray we also need to trace the chief (principal) ray when calculating coefficients for off-axis aberrations. Using the chief and the marginal rays, the contribution of a single conic surface to the aberration coefficient of third-order coma could be written as²⁶

$$\begin{aligned} S_{II} = & -y \left[\left(\frac{u_2 - u_1}{1/n_2 - 1/n_1} \right)^2 \left(\frac{u_2}{n_2} - \frac{u_1}{n_1} \right) \left(\frac{u_{c2} - u_{c1}}{u_2 - u_1} \right) \right. \\ & \left. + k (n_2 u_{c2} - n_1 u_{c1}) \frac{(n_2 u_2 - n_1 u_1)^2}{(n_2 - n_1)^2} \right], \quad (32) \end{aligned}$$

where u_{c1} and u_{c2} are respectively the angle of the incident and refracted chief ray. Note that the angles u_{c1} and u_{c2} are measured with respect to the optical axis.

Similar to our derivation of Eq. (29), we find the contribution to aberration coma from an infinitely thin layer of the GRIN structure:

$$\begin{aligned} \delta S_{II} = & -y(z) \left\{ y_c''(z) \frac{Tn\left(\frac{z}{T}\right)^2 y''(z) [-n'\left(\frac{z}{T}\right) y'(z) + Tn\left(\frac{z}{T}\right) y''(z)]}{n'\left(\frac{z}{T}\right)^2} \right. \\ & + k \left[n'\left(\frac{z}{T}\right) y_c'(z) + Tn\left(\frac{z}{T}\right) y_c''(z) \right] \\ & \left. \times \frac{[n'\left(\frac{z}{T}\right) y'(z) + Tn\left(\frac{z}{T}\right) y''(z)]^2}{Tn'\left(\frac{z}{T}\right)^2} \right\} \delta z, \end{aligned} \quad (33)$$

where y_c is the chief ray height defined by the general ray equation, Eq. (22), for which the input height at the anterior surface is $y_0 = 0$, since in the human eye the aperture stop (iris) approximately coincides with the front surface of the lens, and u_0 is the chief ray angle after the refraction from the anterior surface, $u_0 = u_{c0}$. These initial conditions are reflected in coefficients c_1 and c_2 . Now using Eq. (23) we could also find the chief angle u_c within the GRIN lens. Finally by tracing both marginal and chief rays we get the total third-order coma coefficient of the GRIN lens:

$$\begin{aligned} \sum S_{II} = & -y_0 \left[\left(\frac{u_0 - u_a}{1/n_s - 1/n_{\text{aqu}}} \right)^2 \left(\frac{u_0}{n_s} - \frac{u_a}{n_{\text{aqu}}} \right) \left(\frac{u_{c0} - u_{ca}}{u_0 - u_a} \right) \right. \\ & + k_a (n_s u_{c0} - n_{\text{aqu}} u_{ca}) \frac{(n_s u_0 - n_{\text{aqu}} u_a)^2}{(n_s - n_{\text{aqu}})^2} \\ & + \int_{-T_a}^{T_p} dS_{II} - y(T_p) \left\{ \left[\frac{u_p - u(T_p)}{1/n_{\text{vit}} - 1/n_s} \right]^2 \right. \\ & \times \left[\frac{u_p}{n_{\text{vit}}} - \frac{u(T_p)}{n_s} \right] \left[\frac{u_{cp} - u_c(T_p)}{u_a - u_a} \right] \\ & \left. \left. + k_p [n_{\text{vit}} u_{cp} - n_s u_c(T_p)] \frac{[n_{\text{vit}} u_p - n_s u(T_p)]^2}{(n_{\text{vit}} - n_s)^2} \right\}, \end{aligned} \quad (34)$$

where u_{cp} is the outgoing chief ray angle at the posterior surface, which could be calculated as u_p in Eq. (31), and u_{ca} is the angle of the incident chief ray on the anterior lens surface.

Following the same concept we can calculate aberration coefficients for third-order astigmatism, where the contribution of a single surface has the following form

$$\begin{aligned} S_{III} = & -y \left[\left(\frac{u_2 - u_1}{1/n_2 - 1/n_1} \right)^2 \left(\frac{u_2}{n_2} - \frac{u_1}{n_1} \right) \left(\frac{u_{c2} - u_{c1}}{u_2 - u_1} \right) \right. \\ & \left. + k (n_2 u_{c2} - n_1 u_{c1})^2 \frac{(n_2 u_2 - n_1 u_1)}{(n_2 - n_1)^2} \right] \end{aligned} \quad (35)$$

and the contribution of an infinitely thin layer is

$$\begin{aligned} \delta S_{III} = & -y(z) \left\{ y_c''(z)^2 \frac{Tn\left(\frac{z}{T}\right)^2 y''(z) [-n'\left(\frac{z}{T}\right) y'(z) + Tn\left(\frac{z}{T}\right) y''(z)]}{n'\left(\frac{z}{T}\right)^2} \right. \\ & + k [n'\left(\frac{z}{T}\right) y_c'(z) + Tn\left(\frac{z}{T}\right) y_c''(z)]^2 \\ & \left. \times \frac{[n'\left(\frac{z}{T}\right) y'(z) + Tn\left(\frac{z}{T}\right) y''(z)]^2}{Tn'\left(\frac{z}{T}\right)^2} \right\} \delta z, \end{aligned} \quad (36)$$

and the total third-order astigmatism coefficient of the GRIN lens is

$$\begin{aligned} \sum S_{III} = & -y_0 \left[\left(\frac{u_0 - u_a}{1/n_s - 1/n_{\text{aqu}}} \right)^2 \left(\frac{u_0}{n_s} - \frac{u_a}{n_{\text{aqu}}} \right) \left(\frac{u_{c0} - u_{ca}}{u_0 - u_a} \right) \right. \\ & + k_a (n_s u_{c0} - n_{\text{aqu}} u_{ca})^2 \frac{(n_s u_0 - n_{\text{aqu}} u_a)}{(n_s - n_{\text{aqu}})^2} \\ & + \int_{-T_a}^{T_p} dS_{III} - y(T_p) \left\{ \left[\frac{u_p - u(T_p)}{1/n_{\text{vit}} - 1/n_s} \right]^2 \left[\frac{u_p}{n_{\text{vit}}} - \frac{u(T_p)}{n_s} \right] \right. \\ & \times \left[\frac{u_{cp} - u_c(T_p)}{u_a - u_a} \right]^2 + k_p [n_{\text{vit}} u_{cp} - n_s u_c(T_p)]^2 \\ & \left. \left. \times \frac{[n_{\text{vit}} u_p - n_s u(T_p)]^2}{(n_{\text{vit}} - n_s)^2} \right\}. \end{aligned} \quad (37)$$

In a similar way, the field curvature of a single surface can be achievable as

$$S_{IV} = -n_1 (u_{c1} y - u_1 y_c)^2 \frac{n_2 u_2 - n_1 u_1}{y n_2}, \quad (38)$$

where y_c is the height of the chief ray at the surface. Then for an infinitely thin layer we have

$$\delta S_{IV} = -\frac{[-y_c(z) y'(z) + y(z) y_c'(z)]^2 [n'\left(\frac{z}{T}\right) y'(z) + Tn\left(\frac{z}{T}\right) y''(z)]}{T y(z)} \delta z, \quad (39)$$

and finally for the GRIN lens we have

$$\begin{aligned} \sum S_{IV} = & -n_{\text{aqu}} y_0 u_{ca}^2 \frac{n_s u_0 - n_{\text{aqu}} u_a}{n_s} \\ & + \int_{-T_a}^{T_p} dS_{IV} - n_s [u_c(T_p) y(T_p) \\ & - u(T_p) y_c(T_p)]^2 \frac{n_{\text{vit}} u_p - n_s u(T_p)}{y(T_p) n_{\text{vit}}}. \end{aligned} \quad (40)$$

Despite the advantages of the Seidel theory, the third-order aberration calculations are limited to centered, rotationally symmetric systems, and do not support tilted or decentered elements, such as the crystalline lens in the eye. However, deriving the Seidel aberration coefficients of the GRIN lens in closed form is useful for understanding the nature of aberration compensation inside the GRIN structure. In addition to this, *in vitro* studies of the crystalline lens and its reconstruction based on the experimentally measured lenticular aberrations can benefit from the Seidel aberration representation.

It is worth mentioning that the capability of the geometry-invariant GRIN lens model is not limited to paraxial ray tracing and third-order aberration theory. In future work numerical ray tracing will be developed to calculate Zernike coefficients of the GRIN model lens, which can take the tilt and decenter of the lens into account.

8 Numerical Examples

We present an example of the eye model with the corneal and lenticular shape corresponding to a 40-year-old eye¹⁶ with GRIN profile exponent $p = 3.13$ found in.¹⁴ Figure 2 shows the main optical characteristics of the GRIN lens including the optical power, focal length, back focal length, as well as Seidel aberration coefficients; the lens geometry and GRIN structure parameters are given on the left side. Figure 2 actually

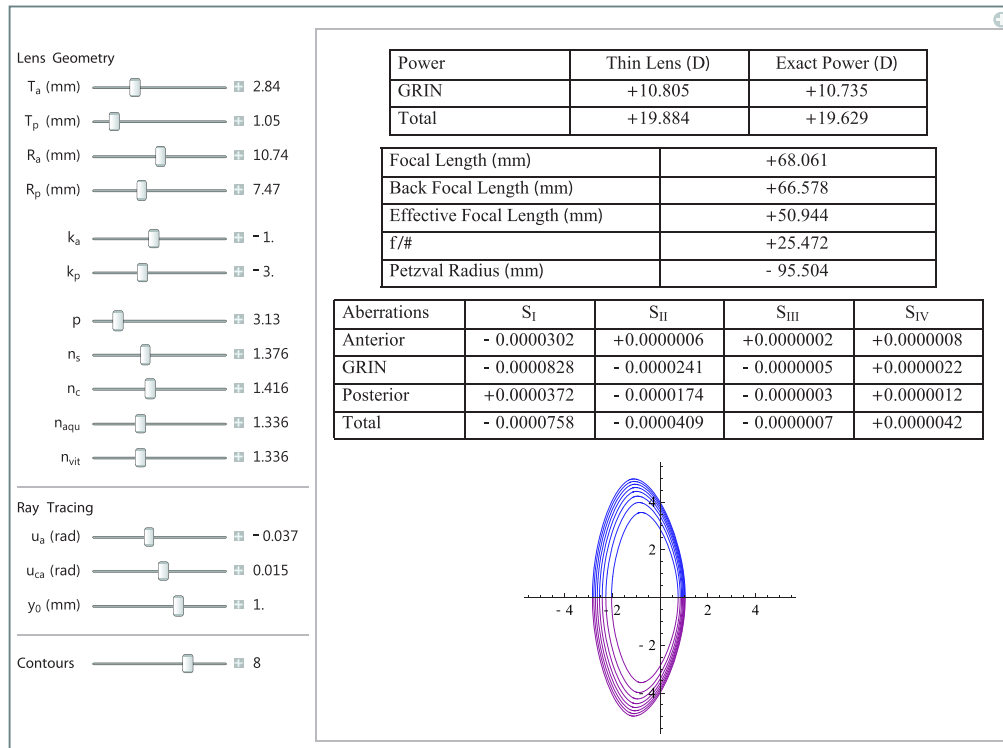


Fig. 2 Optical characteristics of a typical 40-year-old eye (each contour indicates 0.005 change in the refractive index). The image depicts the user interface for the open-source code available from the authors.²⁷

depicts the user interface for the open-source code written by the authors, available at.²⁷ This code incorporates all mathematical expressions presented in this paper.

The optical power of the lens shown in Fig. 2 is based on the thin lens approximation in Eq. (14), and the exact power formula in Eq. (25). It is easy to see that the difference in optical power calculation is less than 1.4%, which indicates that Eq. (14) is useful especially if one wants to determine the exponent p for a given optical power. This can be done by solving Eq. (14) for p , which leads to

$$p = \frac{R_a n_{vit} + R_p (n_{aqu} + FR_a) - n_s (R_a + R_p)}{2[R_a n_{vit} + R_p (n_{aqu} + FR_a) - n_c (R_a + R_p)]}. \quad (41)$$

Knowing the external shape, measuring the optical power of the lens and the surface refractive index n_s , and assuming n_c is based on extensive experimental data, one could determine the GRIN profile exponent p for lenses *in vitro*. This approach provides a practical way to approximate the GRIN profile, which defines all optical characteristics of the lens.

The optical power of the crystalline lens and its age-related changes have been a controversial topic for decades. Many studies (e.g., Ref. 28) show that for an unaccommodated lens, its external surfaces become more curved and therefore more powerful with age. On the other hand, measurements of the total optical power of the eye suggest that the power does not change much with age.²⁹ This lens paradox might be explained, at least in part, by adjusting the center and surface refractive indices of the GRIN structure (n_c and n_s), the axial position of the peak in the refractive index profile (T_a or T_p), the lens axial thickness ($T_a + T_p$), and also the exponent

p .^{16,19,30–32} The latter parameter is the most challenging one to analyze, since calculating the contribution of the GRIN structure to the lens power has not been derived in an easily accessible form.

Pierscionek³² suggested that a slight change in the slope of refractive index in the cortex might compensate the increase in lens curvature and prevent the eye from becoming myopic with age. Using Eq. (14) we can calculate the optical power change in the lens due to an age-related increase in the exponent p . Following a recent study¹⁴ we select three age groups (20-, 40-, and 60-year-olds) with corresponding empirical value for p , see Table 1. To study the effect of p independently from other variables, such radii and central thickness, all three age groups have identical lens geometry. In Fig. 2 we can see that 1 D change in the optical power can be attributed to GRIN profile steepening alone.

It can be seen from Eq. (25) that one can easily adjust other parameters of the lens affecting the lens paradox and take into account their effect due to aging on the lens power. To adjust these parameters in a meaningful way, more experimental

Table 1 Three age groups (20-, 40-, and 60-year old) with corresponding empirical value for p and corresponding powers.

Age (year)	p	Thin lens power (D)	Exact power (D)
20	2.87	20.074	19.815
40	3.13	19.884	19.629
60	4.28	19.359	19.115

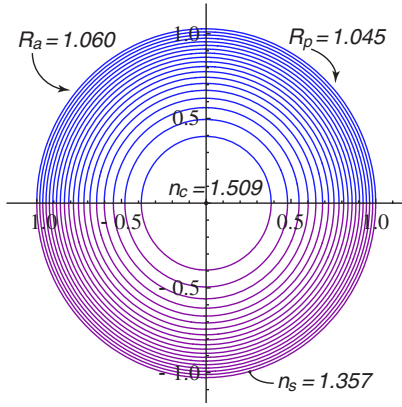


Fig. 3 The octopus eye model (each iso-indicial contour at 0.008 step in the refractive index).

data on the age-related changes in the GRIN structure is required.

The model presented here is not only useful for human eyes, it can also be beneficial for animal eye studies. For example, Fig. 3 shows the octopus eye model based on the experimental data provided by Jagger et al.,³³ where a strictly symmetrical lens was modeled. The original experimental data shows some departure from symmetry, which is taken into account in our model, presented in Fig. 3.

9 Conclusion

The characterization of GRIN lenses by ray-tracing is notoriously difficult and usually requires numerical methods, while only a handful of analytical solutions exist (e.g., Lundberg lens).

In light of this, we introduce and analyze a new class of GRIN lens, which has the following properties. The refractive index distribution is based on the power law defined by the exponent p , which can be adjusted in a continuous manner. The mathematical description of the external surfaces is a standard conicoid of revolution with a higher-order term. Iso-indicial contours feature smooth connection between the anterior and posterior hemispheres. Analytical paraxial ray tracing is possible, which provides expressions for all optical characteristics of the lens and its monochromatic aberrations. The description for aberration coefficients of a thin homogeneous layer is useful for a general GRIN lens description.

A few examples are presented to illustrate the advantage of this GRIN mode with special emphasis given to the thin lens approximation formula. The latter is very accurate, and can be used to analyze the role of exponent p in lens paradox. One could also determine the exponent p for a given optical power measured experimentally *in vitro*.

The interior iso-indicial contours mimic the external shape of the lens, which leads to invariant geometry of the GRIN structure. Due to this strong coupling between the external shape of the lens and its GRIN structure, one could study the changes in aberrations with accommodation. A dispersion model and chromatic aberrations of the lens will be derived in future work.

The new GRIN lens model can be used for other types of eyes, even for such an extreme case as the octopus eye. A user-friendly software incorporating all mathematical expressions is available from the authors.²⁷

Appendix: Coefficient Definitions

$$\mathcal{F}_1 = {}_2F_1\left(\frac{-1+2p-\alpha}{4p}, \frac{-1+2p+\alpha}{4p}; 1 - \frac{1}{2p}; \frac{n_c - n_s}{n_c}\right)$$

$$\mathcal{F}_2 = {}_2F_1\left(\frac{1+2p-\alpha}{4p}, \frac{1+2p+\alpha}{4p}; 1 + \frac{1}{2p}; \frac{n_c - n_s}{n_c}\right)$$

$$\mathcal{F}_3 = {}_2F_1\left(\frac{-1+6p+\alpha}{4p}, \frac{-1+6p-\alpha}{4p}; 2 - \frac{1}{2p}; \frac{n_c - n_s}{n_c}\right)$$

$$\mathcal{F}_4 = {}_2F_1\left(\frac{1+6p-\alpha}{4p}, \frac{1+6p+\alpha}{4p}; 2 - \frac{1}{2p}; \frac{n_c - n_s}{n_c}\right)$$

$$\mathcal{F}_5 = {}_2F_1\left(\frac{1+2p-\alpha}{4p}, \frac{1+6p-\alpha}{4p}; 1 + \frac{1}{2p}; \frac{n_c - n_s}{n_c}\right)$$

$$\mathcal{F}_6 = {}_2F_1\left(\frac{-1+6p+\beta}{4p}, \frac{1+6p-\beta}{4p}; 2 - \frac{1}{2p}; \frac{n_c - n_s}{n_c}\right)$$

$$\mathcal{F}_7 = {}_2F_1\left(\frac{1+6p-\beta}{4p}, \frac{1+6p+\beta}{4p}; 2 + \frac{1}{2p}; \frac{n_c - n_s}{n_c}\right)$$

$$\mathcal{F}_8 = {}_2F_1\left(\frac{1+2p-\beta}{4p}, \frac{1+2p+\beta}{4p}; 1 + \frac{1}{2p}; \frac{n_c - n_s}{n_c}\right)$$

$$\mathcal{F}_9 = {}_2F_1\left(\frac{-1+2p+\beta}{4p}, \frac{-1+2p-\beta}{4p}; 1 - \frac{1}{2p}; \frac{n_c - n_s}{n_c}\right)$$

$$\mathcal{F}_{10} = {}_2F_1\left(\frac{-1+2p-\beta}{4p}, \frac{-1+2p+\beta}{4p}; 1 - \frac{1}{2p}; \frac{n_c - n_s}{n_c}\right)$$

$$\gamma_1 = \frac{n_c - n_s}{n_c} \frac{(1+2p)^2 - \alpha^2}{8p+4}$$

$$\gamma_2 = \frac{n_c - n_s}{n_c} \frac{(1-2p)^2 - \alpha^2}{8p-4}$$

$$\gamma_3 = \frac{n_c - n_s}{n_c} \frac{(1+2p)^2 - \beta^2}{8p+4}$$

$$\gamma_4 = \frac{n_c - n_s}{n_c} \frac{(1-2p)^2 - \beta^2}{8p-4}$$

$$A_{\text{GRIN}} = \frac{n_s[\gamma_4 T_a(\gamma_1 \mathcal{F}_4 + \mathcal{F}_5) \mathcal{F}_6 + \gamma_2 T_p \mathcal{F}_3(\gamma_3 \mathcal{F}_7 + \mathcal{F}_8)]}{T_a T_p [\gamma_2 \mathcal{F}_2 \mathcal{F}_3 - \mathcal{F}_1(\gamma_1 \mathcal{F}_4 + \mathcal{F}_5)]}$$

$$A_a = \frac{\gamma_4 T_a \mathcal{F}_2 \mathcal{F}_6 + T_p \mathcal{F}_1(\gamma_3 \mathcal{F}_7 + \mathcal{F}_8)}{T_p [\mathcal{F}_1(\gamma_1 \mathcal{F}_4 + \mathcal{F}_5) - \gamma_2 \mathcal{F}_2 \mathcal{F}_3]}$$

$$A_p = \frac{\gamma_2 T_p \mathcal{F}_3 \mathcal{F}_8 + T_a(\gamma_1 \mathcal{F}_4 + \mathcal{F}_5) \mathcal{F}_9}{T_a [\mathcal{F}_1(\gamma_1 \mathcal{F}_4 + \mathcal{F}_5) - \gamma_2 \mathcal{F}_2 \mathcal{F}_3]}$$

$$A_d = \frac{T_p \mathcal{F}_1 \mathcal{F}_8 + T_a \mathcal{F}_2 \mathcal{F}_9}{(\mathcal{F}_1 \gamma_1 \mathcal{F}_4 + \mathcal{F}_5) - \gamma_2 \mathcal{F}_2 \mathcal{F}_3}$$

$$B_f = -\frac{T_a \mathcal{F}_{10} (\gamma_1 \mathcal{F}_4 + \mathcal{F}_5) + \gamma_2 T_p \mathcal{F}_3 \mathcal{F}_8}{T_a (\gamma_2 \mathcal{F}_2 \mathcal{F}_3 - \gamma_1 \mathcal{F}_1 \mathcal{F}_4 - \mathcal{F}_1 \mathcal{F}_5)}$$

$$+ \frac{n_s - n_{\text{aqu}}}{n_s R_a} \frac{T_a \mathcal{F}_{10} \mathcal{F}_2 + T_p \mathcal{F}_1 \mathcal{F}_8}{\gamma_2 \mathcal{F}_2 \mathcal{F}_3 - \gamma_1 \mathcal{F}_1 \mathcal{F}_4 - \mathcal{F}_1 \mathcal{F}_5}$$

Acknowledgments

The authors would like to thank Chris Dainty for his valuable comments. This research was supported by Science Foundation Ireland under grant 07/IN.1/1906.

References

- G. Beadie et al., "Optical properties of a bio-inspired gradient refractive index polymer lens," *Opt. Express* **16**(6), 11540–11547 (2008).
- R. K. Luneburg, *Mathematical Theory of Optics* Brown University, Providence, RI (1944).
- A. Gullstrand, *Hemholtz's Handbuch der Physiologischen Optik*, 3rd ed., English translation edited by J. P. Southall Ed., Optical Society of America, Vol. **1**, Appendix II, pp. 351–352 (1924).
- J. W. Blaker, "Toward an adaptive model of the human eye," *J. Opt. Soc. Am. A* **70**(2), 220–223 (1980).
- D. Y. C. Chan et al., "Determination and modeling of the 3-D gradient refractive indices in crystalline lenses," *Appl. Opt.* **27**(5), 926–931 (1988).
- G. Smith, B. K. Pierscionek, and D. A. Atchison, "The optical modelling of the human lens," *Ophthalmic Physiol. Opt.* **11**(4), 359–369 (1991).
- H. L. Liou and N. A. Brennan, "Anatomically accurate, finite model eye for optical modeling," *J. Opt. Soc. Am. A* **14**(8), 1684–1695 (1997).
- J. Liang et al., "Objective measurement of wave aberrations of the human eye with the use of a hartmann-shack wave-front sensor," *J. Opt. Soc. Am. A* **11**(7), 1949–1957 (1994).
- C. E. Jones et al., "Refractive index distribution and optical properties of the isolated human lens measured using magnetic resonance imaging (MRI)," *Vis. Res.* **45**(18), 2352–2366 (2005).
- S. Kasthurirangan et al., "In vivo study of changes in refractive index distribution in the human crystalline lens with age and accommodation," *Invest. Ophthalmol. Vis. Sci.* **49**(6), 2531–2540 (2008).
- D. Vazquez et al., "Tomographic method for measurement of the gradient refractive index of the crystalline lens. II. The rotationally symmetrical lens," *J. Opt. Soc. Am. A* **23**(10), 2551–2565 (2006).
- A. de Castro et al., "Three-dimensional reconstruction of the crystalline lens gradient index distribution from OCT imaging," *Opt. Express* **18**(21), 21905–21917 (2010).
- M. Hoshino et al., "Optical properties of in situ eye lenses measured with x-ray talbot interferometry: a novel measure of growth processes," *PLoS One* **6**(9), e25140 (2011).
- R. Navarro, F. Palos, and L. González, "Adaptive model of the gradient index of the human lens. I. formulation and model of aging ex vivo lenses," *J. Opt. Soc. Am. A* **24**(8), 2175–2185 (2007).
- G. Smith, D. A. Atchison, and B. K. Pierscionek, "Modeling the power of the aging human eye," *J. Opt. Soc. Am. A* **9**(12), 2111–2117 (1992).
- A. V. Goncharov and C. Dainty, "Wide-field schematic eye models with gradient-index lens," *J. Opt. Soc. Am. A* **24**(8), 2157–2174 (2007).
- G. Smith and D. Atchison, "Equivalent power of the crystalline lens of the human eye: comparison of methods of calculation," *J. Opt. Soc. Am. A* **14**(10), 2537–2546 (1997).
- P. J. Sands, "Third-order aberrations of inhomogeneous lens," *J. Opt. Soc. Am. A* **60**(11), 1436–1443 (1970).
- J. A. Díaz, C. Pizarro, and J. Arasa, "Single dispersive gradient-index profile for the aging human lens," *J. Opt. Soc. Am. A* **25**(1), 250–261 (2008).
- S. Nakao et al., "Model of refractive indices in the human crystalline lens," *Jpn. J. Clin. Ophthalmol.* **23**, 903–906 (1969).
- B. K. Pierscionek and D. Y. C. Chan, "Refractive index gradient of human lenses," *Optom. Vis. Sci.* **66**(12), 822–829 (1989).
- H. T. Kasprzak, "New approximation for the whole profile of the human crystalline lens," *Ophthalmic Physiol.* **20**(1), 31–43 (2000).
- R. Urs et al., "Age-dependent Fourier model of the shape of the isolated ex vivo human crystalline lens," *Vis. Res.* **50**(11), 1041–1047 (2010).
- S. Dorić and N. Renaud, "Analytical expressions for the paraxial parameters of a single lens with a spherical distribution of refractive index," *Appl. Opt.* **31**(25), 5197–5200 (1992).
- W. J. Smith, *Modern Optical Engineering* McGraw-Hill, New York (2000).
- B. N. Begunov et al., *Optical Instrumentation: Theory and Design*. Mir, Moscow (1988).
- The geometry-invariant lens computational code. This is a computable document format (CDF) for the equations presented in the paper. Our source CDF code can be accessed via Mathematica, the computational software developed by Wolfram Research (Oct. 2011), <http://optics.nuigalway.ie/people/mehdiB/CDF.html>
- N. Brown, "The change in lens curvature with age," *Exp. Eye Res.* **19**(2), 175–183 (1974).
- H. Saunders, "A longitudinal study of the age-dependence of human ocular refraction I. Age-dependent changes in the equivalent sphere," *Ophthalmic Physiol. Opt.* **6**(1), 39–46 (1986).
- R. P. Hemenger, L. F. Garner, and C. S. Ooi, "Changes with age of the refractive index gradient of the human ocular lens," *Invest. Ophthalmol. Vis. Sci.* **36**(3), 703–707 (1995).
- G. Smith and B. K. Pierscionek, "The optical structure of the lens and its contribution to the refractive status of the eye," *Ophthalmic Physiol. Opt.* **18**(1), 21–29 (1998).
- B. K. Pierscionek, "Presbyopia—effect of refractive index," *Clin. Exp. Optom.* **73**(1), 23–30 (1990).
- W. S. Jagger and P. J. Standsl, "A wide-angle gradient index optical model of the crystalline lens and eye of the octopus," *Vis. Res.* **39**(17), 2841–2852 (1999).